

# Effects of Process Parameters on Superplastic Forming of a License Plate Pocket Panel

**M. H. Shojaeefard**

Department of Automotive Engineering,  
University of Science and Technology, Tehran, Iran  
E-mail: mhshf@iust.ac.ir

**A. Khalkhali\***

Department of Automotive Engineering,  
University of Science and Technology, Tehran, Iran  
E-mail: ab\_khalkhali@iust.ac.ir

\*Corresponding author

**E. Miandoabchi**

Department of Automotive Engineering,  
University of Science and Technology, Tehran, Iran  
E-mail: el\_miandoabchi@auto.iust.ac.ir

Received: 3 March 2013, Revised: 3 December 2013, Accepted: 27 January 2014

**Abstract:** Superplastic forming (SPF) is a manufacturing process utilized in the automotive industry to produce complex geometry aluminum or magnesium alloy components which cannot be fabricated at room temperature. The die entry radius and the friction coefficient at the sheet-die interface greatly influence the metal flow during the SPF process. This paper investigates the effects of the die entry radius and the interfacial friction coefficient on the required forming time and thickness distribution of a superplastic formed vehicle closure panel. A commercial finite element software, ABAQUS/Implicit, is applied to simulate forming of AA5083 aluminum alloy into a license plate pocket panel. The results indicate that for a fixed friction coefficient, increasing the entry radius reduces the forming time and enhances the formed part quality, in terms of thickness distribution. It is also shown that the lower the friction coefficient, the higher the sensitivity of the forming time to the die entry radius variations.

**Keywords:** Die Entry Radius, Finite Element Method, Forming Time, Superplastic Forming, Thinning Factor

**Reference:** Shojaeefard, M. H., Khalkhali, A., and Miandoabchi, E., "Effects of Process Parameters on Superplastic Forming of a License Plate Pocket Panel", Int J of Advanced Design and Manufacturing Technology, Vol. 7/No. 2, 2014, pp. 25-33.

**Biographical notes:** **M. H. Shojaeefard** received his PhD in Mechanical Engineering from Birmingham University in 1987. He is currently Professor at the Departments of Mechanical and Automotive Engineering, University of Science and Technology, Tehran, Iran. His current research focuses on Fluid Mechanics, Turbomachines, Gas Turbine and Design of Machines. **A. Khalkhali** is Associate Professor of Automotive Engineering at the University of Science and Technology, Tehran, Iran. His current research interest includes Automobile Body Structure Design and Analysis, Finite Element Analysis (FEM) and application of Neural Networks and Optimization in Engineering Design. **E. Miandoabchi** received his MSc in Automotive Engineering from Iran University of Science and Technology.

## 1 INTRODUCTION

High fuel cost has led to the use of lightweight materials in the automotive industry. This may be achieved by applying aluminum or magnesium alloys as a replacement for steel in the automobile body structure and closure panels. Such alloys have low formability at room temperature. Superplastic forming (SPF) is a manufacturing method to form lightweight alloys into complex shapes at high temperatures using gas pressure. Superplastic materials are considered a unique class of solids which can withstand large strains before failure when they are deformed under specific conditions. This type of materials may experience elongations beyond 1000% at elevated temperatures and low strain rates [1].

SPF process is applied in the automotive and aerospace industries, architecture, rail transport and in the medical fields. Due to the high sensitivity of the flow stress to the strain rate, this process is performed at low strain rates. Therefore, SPF is carried out slower than conventional forming techniques and this may cause longer forming times. Near net shape forming, fabricating multiple components in one stage, little spring-back and tooling cost saving are some advantages of SPF over conventional stamping processes. However, longer forming times and nonuniformity of the products are considered as disadvantages of SPF process.

Splitting at die entry region is a prevailing failure mode in SPF of sheet materials at high strain rates [2-5]. Compressive stress created during sliding of the sheet over the die entry radius, leads to thinning. Friction at the sheet-die interface affects local thinning [5].

Effects of die geometry and the sheet-die interface friction on strain localization were first investigated by Ghosh and Hamilton [6]. Thinning in a rectangular tray was studied using finite element analysis by Khaleel, Johnson, and Smith [7]. Thinning of AA5083 sheet in a rectangular die was studied by Luckey, Friedman and Weinmann using two different finite element softwares [8]. Thinning of superplastic formed circular and elliptical AL-Li alloy parts was investigated in [9-10]. Geometric analysis of thinning during superplastic forming of prismatic die shapes was presented in [11]. Effects of three material models on necking predictions for the superplastic gas-blow forming of a structural component were studied in [12]. Thickness distribution of superplastic formed aircraft skin components was investigated in [13]. The post-formed properties, thinning, of a decklid inner panel formed using quick plastic forming (QPF) was investigated experimentally by Verma and Carter [14].

The effect of sheet/die friction on thickness distribution of a decklid inner panel formed using QPF was studied in [15]. Effects of interfacial friction distribution on the

integrity of superplastic formed parts were studied in [16]. SPF of titanium alloy sheet was investigated in [17] and the forming characteristics of thickness distribution and forming time with and without die entry radius and friction coefficient were analyzed. Thickness distribution of superplastic formed titanium-based domes was studied in [18].

The possibility of reducing the SPF process forming time by designing variable strain rate paths was addressed in [19-21]. An optimal variable strain rate forming path was developed in [22] with the aim of reducing forming time. QPF of an AA5083 aluminum alloy license plate pocket at 450°C was studied in [5], [23]. SPF of an AZ31 magnesium alloy license plate pocket at 470°C was investigated in [24]. Effects of forming parameters such as fluid pressure, die entry radius and the interfacial friction coefficient on hydroforming of St14 steel sheet were studied by Zareh, Gorji, Bakhshi, and Nourouzi [25].

These studies mainly focused on the influences of the sheet-die interface friction on the forming time and the formed panel thickness distribution. None of these studies addressed the effects of the die entry radius and the interfacial friction coefficient simultaneously on the required forming time and thickness distribution of the formed license plate pocket panel. The aim of this paper is to investigate the effects of die entry radius and friction coefficient on SPF of a lightweight alloy license plate pocket panel with a complex geometry. Numerical simulation of SPF of the panel is conducted using commercial finite element software, ABAQUS.

## 2 MATERIAL CONSTITUTIVE MODEL

The power-law model in Eq. (1) is widely applied in the industrial applications:

$$\sigma = K \dot{\epsilon}^m \epsilon^n \quad (1)$$

Where  $\sigma$  is the effective flow stress,  $\dot{\epsilon}$  is the effective strain rate,  $\epsilon$  is the effective strain,  $m$  is sensitivity of the flow stress to the strain rate and  $n$  is the strain hardening component. The power law constitutive model coefficients for the AA5083 aluminum alloy at 475°C are considered as  $K= 187.7$  MPa,  $m= 0.39$  and  $n=0.088$  [8]. At high temperatures, strain component may be neglected and Eq. (1) can be written in the following form:

$$\sigma = K \dot{\epsilon}^m \quad (2)$$

### 3 NUMERICAL SIMULATION

The cross section geometry at the die mid-section, which is taken from [23], is presented in Fig. 1.

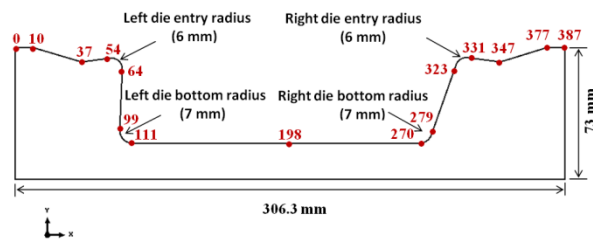


**Fig. 1** The cross section geometry at the die mid-section the numbers in red show positions (mm) relative to the edge of the left die flange

The length and width of the die are, respectively, 761 mm and 306.3 mm. Thus, the license plate pocket can be considered as an infinitely long rectangular box [23] enabling plain strain 2D modelling of the mid-section. Previous studies by Luckey et al., [26] show that 2D modelling with layered solid elements can predict sheet thinning better than 3D modelling. Finite element software, ABAQUS/Implicit, was used to implement finite element simulation. Modelling of the AA5083 sheet with a thickness of 1.2 mm was carried out using 4 layers; each of which contained 554 CPE4R quadrilateral solid elements.

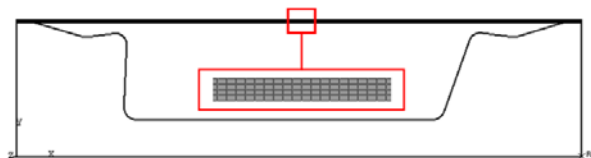


**Fig. 2** 2D finite element model of the die and the sheet showing the layered solid elements of the sheet

Fig. 2 shows 2D FE model of the die and the metal sheet. The nodes located at the left and right edges of the sheet were constrained in all directions to simulate the clamping of the sheet. An isotropic Coulomb friction model at the die-sheet interface was employed in simulations. This model relates the critical shear stress ( $\tau_{crit}$ ) across an interface at which sliding occurs, friction coefficient ( $\mu$ ) and the forming pressure ( $P$ ):

$$\tau_{crit} = \mu P \tag{3}$$

A target maximum effective strain rate of  $0.0025s^{-1}$  was maintained during all simulations by means of ABAQUS pressure control algorithm, which is detailed in the next section. The maximum allowable pressure was 2 MPa.

### 4 NUMERICAL PRESSURE CONTROL ALGORITHM

A pressure control algorithm internal to ABAQUS [27] was employed to maintain a target for maximum effective strain rate of  $0.0025s^{-1}$  in the sheet elements. This control algorithm was performed in ABAQUS by means of solution dependent amplitude. For each time increment the pressure was calculated as follows: the maximum equivalent strain rate ( $\dot{\epsilon}_{max}$ ) was determined for the elements, then, the ratio of the maximum equivalent strain rate to the target strain rate was computed (Eq. (4)).

$$r = \dot{\epsilon}_{max} / \dot{\epsilon}_{target} \tag{4}$$

The following logic is used to adjust the pressure for the next increment:

If	$0.2 \leq r < 0.5$	Then	$p^{new} = 1.5p^{old}$
If	$0.5 \leq r < 0.8$	Then	$p^{new} = 1.2p^{old}$
If	$0.8 \leq r < 1.5$	Then	$p^{new} = p^{old}$
If	$1.5 \leq r < 3.0$	Then	$p^{new} = 0.834p^{old}$

If the ratio is less than 0.2 or greater than 3, the increment is restarted with a pressure which is computed as shown below:

If	$r < 0.2$	Then	$p^{new} = 2p^{old}$
If	$r > 3.0$	Then	$p^{new} = 0.5p^{old}$

### 5 RESULTS AND DISCUSSION

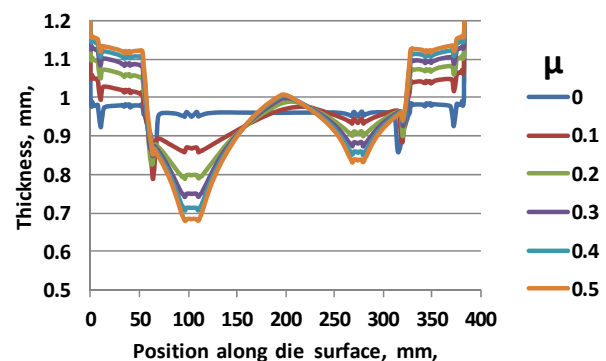


**Fig. 3** FE-predicted thickness profiles at the mid-section of the formed panel with  $R=6$  mm for different friction conditions

In Fig. 3 it could be observed that with  $\mu=0$ , the peak thinning occurs just below the die entry radius because of the superimposed compressive stresses and bending effects at that region. In the case of idealized

lubrication, away from the die entry region, little deviation is observed in the thickness value because contact surface between the sheet and the die has no effect on stretching the material and constant material feed is provided. By increasing the friction coefficient, considerable deviation is observed in the formed part thickness value because of the resistance to material stretching which occurs when the sheet touches the die surface.

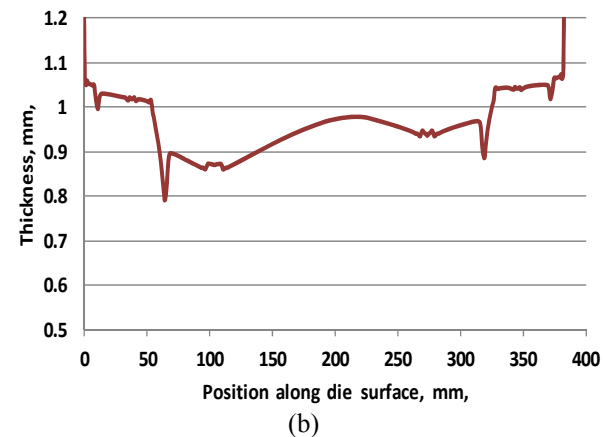
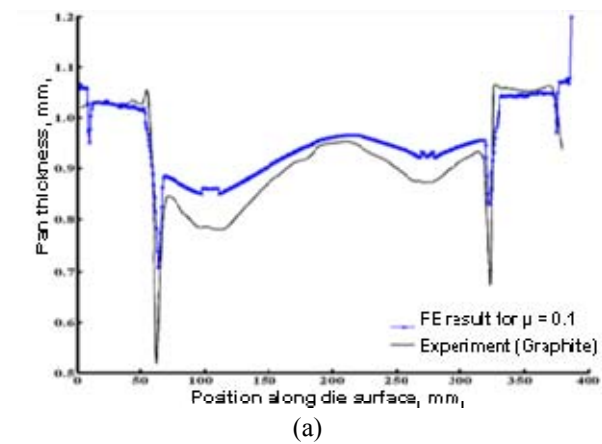


**Fig. 4** a) FE-predicted thickness profile at the mid-section of the formed panel with  $\mu=0.1$  (blue) [23], and compared with that obtained experimentally (black) using graphite as a lubricant, b) FE-predicted thickness profile (red) obtained in this study with  $\mu=0.1$

A comparison between the predicted thickness profile at the mid-section of the license plate pocket formed with  $\mu=0.1$  at  $450^{\circ}\text{C}$  in [23], and that obtained experimentally by General Motors company using graphite as a lubricant, is presented in Fig. 4-a. Thickness profile of the formed panel, obtained in the present study, with  $\mu=0.1$  and a forming temperature of  $475^{\circ}\text{C}$  is also shown in Fig. 4-b.

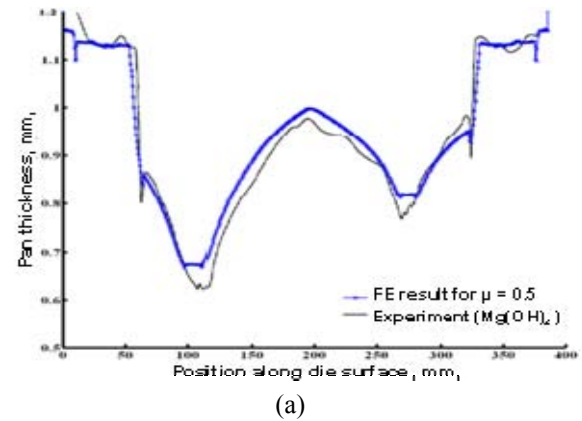


**Fig. 5** a) FE-predicted thickness profile at the mid-section of the formed panel with  $\mu=0.5$  (blue) [23], and compared with that obtained experimentally (black) using graphite as a lubricant, b) FE-predicted thickness profile (red) obtained in this study with  $\mu=0.5$

Figure 5 shows the FE-predicted thickness profiles at the mid-section of the formed panel with  $R=6$  mm for different friction conditions. The predicted thickness profiles agree qualitatively well with those obtained with the same die geometry by Jarrar, Hector, Khraisheh, and Bower [23]. It should be noted that the sheet thickness and material are the same as those used in Jarrar's work, but their study used a different superplastic material model as well as a different forming temperature of  $T=450^{\circ}\text{C}$ . Moreover, in the present study, the ABAQUS built-in pressure control algorithm is employed to maintain a target effective strain rate of  $0.0025\text{s}^{-1}$  whereas, the pressure profile used in Jarrar's study was suggested from previous experiments.

Figure 5 compares the FE predicted thickness profiles of the mid-section of the formed panel with  $\mu=0.5$  and those obtained experimentally by General Motors company using  $\text{Mg}(\text{OH})_2$  as a lubricant. It is observed that the shape of the FE-predicted thickness profiles in Figs. 4 and 5, generally follows the experimental profiles.

Local thinning at the die entries from experiment is more severe than the corresponding FE predictions. This difference is due to neck development in the experiments. The thinning factor, which is defined as the ratio of the minimum thickness of the formed part ( $t_{Min}$ ) to its average thickness ( $t_{Avg}$ ), is usually used to evaluate the uniformity of the thickness distribution of the product. The higher the thinning factor, the lower is the deviation in the product thickness distribution. To investigate the effects of the die entry radius and the interfacial friction coefficient on the required forming time and thickness uniformity of the fully formed part, the die entry radius ( $R$ ) has been varied from 4 to 8 millimeters with increments of 1 millimeter where the friction coefficient ( $\mu$ ) has been varied from 0.1 to 0.5 with increments of 0.1 resulting in 25 different combinations of die geometry and friction condition. The die bottom radius has been kept constant during the simulations and it has been assumed that both the left and the right die entries have the same radius ( $R_A=R_B$ ). Figure 6 shows the thinning factors calculated for these combinations.

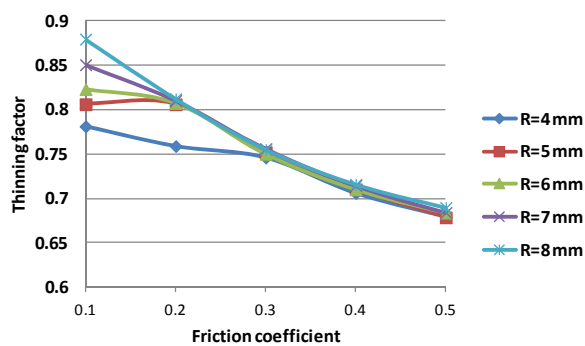


Fig. 6 Effect of the friction coefficient variation on the required forming time, for different values of the die entry radius

From Fig. 8, the following results may be concluded:

- For a fixed friction coefficient, the larger the entry radius, the higher is the thinning factor. This is due to the fact that increasing the entry radius decreases the compressive stress developed in the sheet and reduces local thinning, and accordingly, leads to a more uniform thickness distribution [5].
- For a fixed entry radius, increasing the friction coefficient causes more deviation in the formed part thickness value due to increasing the resistance to material stretching.
- With low friction coefficients, sensitivity of the thinning factor to the die entry radius variations is high; this is because with lower friction coefficients, more material is allowed

to flow from the entry region, resulting in the peak thinning to occur at that region [5], [23], [24] (between 54 and 64 mm along the die surface).

Figure 7 illustrates the predicted thickness profile of the mid-section of the formed panel with  $\mu=0.1$ , for different values of the die entry radius. It could be observed that the die entry radius variation greatly affects the peak thinning.

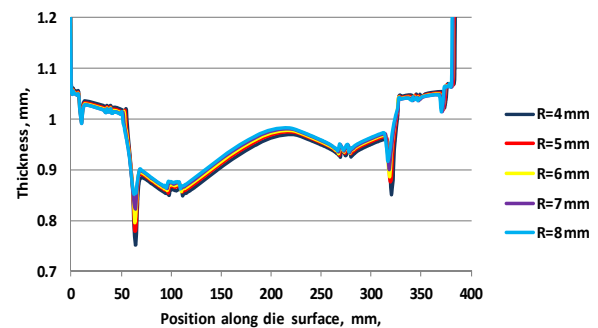


Fig. 7 FE- predicted thickness profiles of the mid-section of the formed panel with  $\mu=0.1$  for different values of the die entry radius

- With higher friction coefficients, less material is permitted to flow from the entry region. Therefore, thinning at that region is reduced and the peak thinning occurs at the die bottom radius region since it is the last region to touch the die surface.

Effect of the die entry radius on the predicted thickness profile of the mid-section of the panel formed with  $\mu=0.5$  is presented in Fig. 8. It could be seen that the value of the die entry radius has minimal effect on the final part thickness distribution. Since the die bottom radius has been assumed to be constant, it has no effect on the peak thinning occurring at the die bottom radius region.

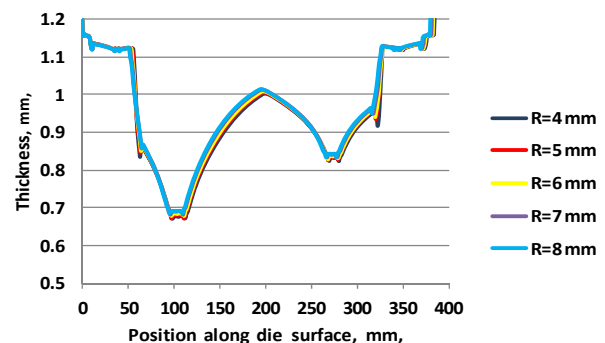
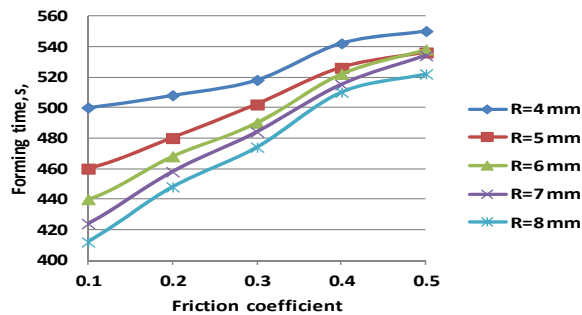


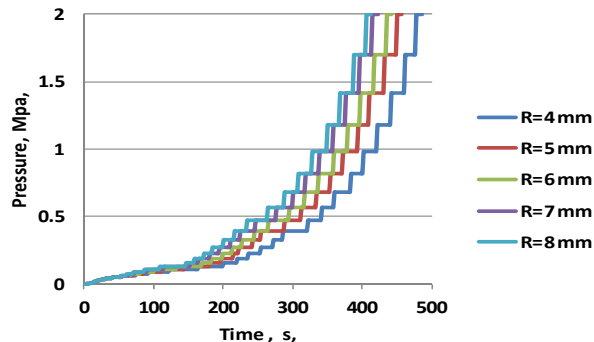
Fig. 8 FE-predicted thickness profiles of the mid-section of the formed panel with  $\mu=0.5$  for different values of the die entry radius

Effect of the friction coefficient variation on the required forming time, for different values of the die entry radius, is depicted in Fig. 9. The following results can be deduced from Fig. 9:

- For a fixed friction coefficient, the larger the entry radius, the lower is the forming time. This can be attributed to the fact that with a larger entry radius, the sheet can make contact with the die bottom surface earlier, and accordingly, fill the die cavity faster.



**Fig. 9** Effect of the friction coefficient variation on the required forming time, for different values of the entry radius



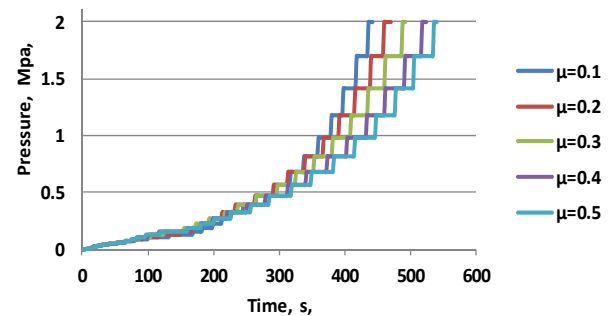
**Fig. 10** Pressure profiles calculated by the ABAQUS pressure control algorithm for a target strain rate of  $0.0025s^{-1}$  with  $\mu=0.1$  for different values of the die entry radius

Figure 10 shows the pressure profiles computed by the ABAQUS internal pressure control algorithm for a target strain rate of  $0.0025s^{-1}$  with  $\mu=0.1$  for different values of the die entry radius.

- From Fig. 10 it could be observed that for a given friction coefficient, a larger entry radius leads to a higher forming pressure, this is because although with a larger entry radius the sheet touches the die bottom surface earlier, the contact between the sheet and the bottom surface of the die and its sidewalls restricts the metal flow, resulting in giving rise to the forming pressure needed to maintain constant strain rate deformation.

- For a fixed entry radius, the higher the friction coefficient, the longer is the forming time. This is due to the fact that by increasing the friction coefficient, the resistance to material stretching increases and this leads to a longer forming time.

Figure 11 illustrates the pressure profiles calculated by the ABAQUS pressure control algorithm for a target strain rate of  $0.0025s^{-1}$  with  $R=6$  mm, for different values of the friction coefficient.

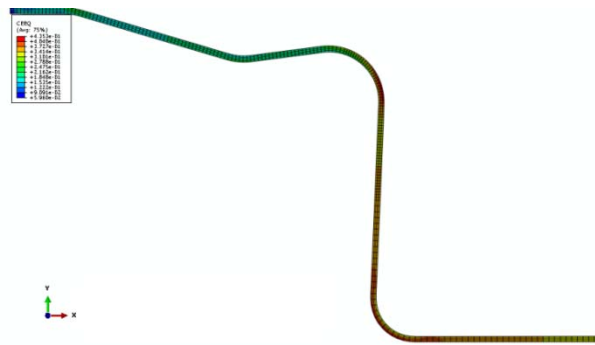


**Fig. 11** Pressure profiles calculated by the ABAQUS pressure control algorithm for a target strain rate of  $0.0025s^{-1}$  with an entry radius of 6 mm for different values of the friction coefficient ( $\mu$ )

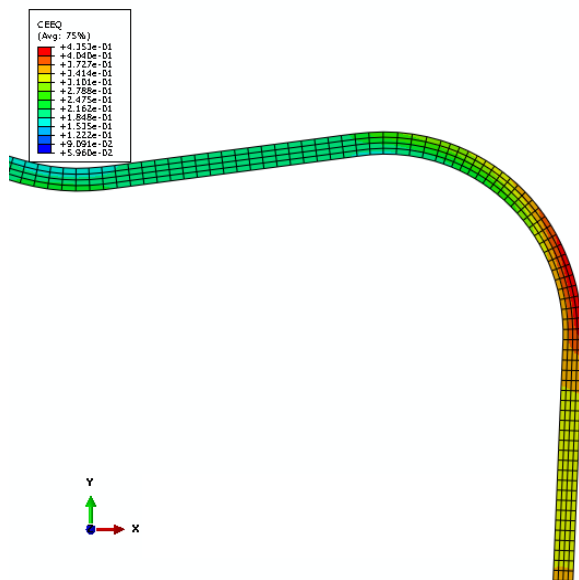
- From Fig. 11 it could be observed that the forming pressure decreases with increasing the friction coefficient. This is because by increasing the friction force, the metal flows into those regions of the sheet which are not in contact with the die, so that the thickness in those regions decreases, and accordingly, the forming pressure needed to maintain the target strain rate decreases.
- With lower friction coefficients, sensitivity of the forming time to the die entry radius variations is high. With higher friction coefficients, sensitivity of the forming time to the entry radius variations is low due to the near sticking condition [16]. For instance, with  $\mu=0.1$ , increasing the entry radius from 4 to 8 millimeters, leads to an 18 percent reduction in the forming time, whereas with  $\mu=0.5$  only a 5 percent reduction in the forming time can be achieved by increasing the entry radius.
- A minimum forming time of 412 seconds can be attained with  $R=8$  mm and  $\mu=0.1$ . Partial views of the effective strain distribution through the thickness of the panel formed with this combination of process parameters are presented in Fig. 12.

In Fig. 12, it could be seen that the minimum thickness occurs at the die entry region. Thinning ( $t_{Min}/t_0$ ) and thinning factor ( $t_{Min}/t_{Avg}$ ) of the formed panel (whose left part is shown), are respectively, 0.71 and 0.88.

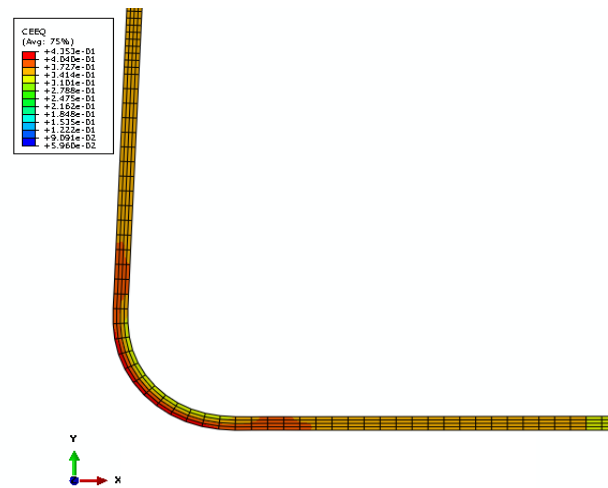
- With  $R=4$  mm and  $\mu=0.5$ , the required forming time is maximum (550s). Partial views of the effective strain distribution through the thickness of the panel formed with this combination of process parameters are presented in Fig. 13.



(a)



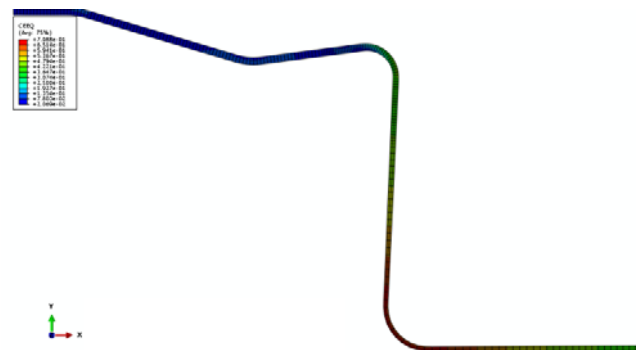
(b)



(c)

**Fig. 12** a) Partial views of the effective strain distribution for a fully formed license plate pocket with a die entry radius of 8 mm and  $\mu=0.1$ , b) Magnified regions of the die entry region, c) Magnified regions of the die bottom radius region

In Fig 13, it is observed that the minimum thickness occurs at the die bottom radius. Thinning ( $t_{Min}/t_0$ ) and thinning factor ( $t_{Min}/t_{Avg}$ ) of the formed panel (whose left part is shown), are, respectively, 0.56 and 0.68.



(a)

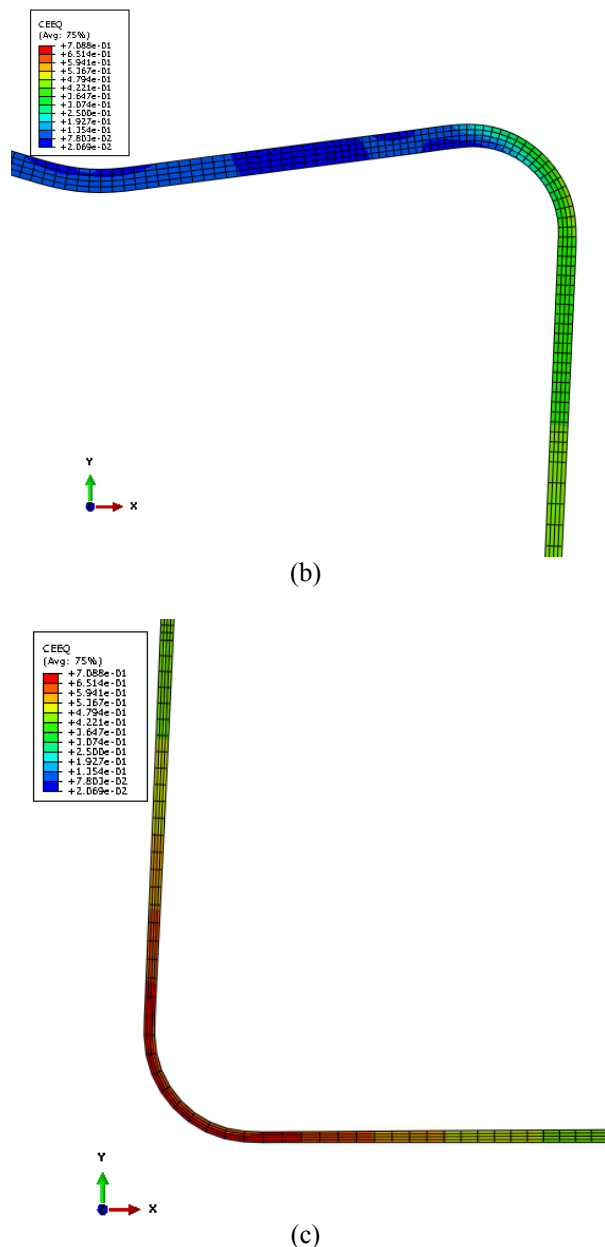


**Fig. 13** a) Partial view of the effective strain distribution for a license plate pocket formed with a die entry radius of 4 mm and  $\mu=0.5$ , b) Magnified regions of the die entry radius, c) Magnified regions of the die bottom radius

## 6 CONCLUSION

2D finite element simulation of superplastic forming of AA5083 aluminum alloy into a vehicle license plate pocket panel was carried out in this study. In order to study the effects of the die entry radius and the interfacial friction coefficient on the required forming time and thickness distribution of the product, a set of

finite element simulations of SPF of the panel with different combinations of die geometry and friction coefficient was conducted.

It was shown that with lower friction coefficients, sensitivity of the formed part thinning factor to the die entry radius variations is high. It was also concluded that a larger die entry radius along with a lower friction coefficient, leads to a shorter forming time and a more uniform final part thickness distribution.

## REFERENCES

- [1] Luckey, G., Friedman, P., and Weinmann, K., "Design and experimental validation of a two-stage superplastic forming die," *Journal of materials processing technology*, Vol. 209, No. 4, 2009, pp.2152-2160.
- [2] Krajewski, P. E., "The Effect of Lubrication on QPF Formability," *Trends in Materials and Manufacturing Technologies for Transportation Industries and Powder Metallurgy Research and Development in the Transportation*, TMS, Warrendale, PA, 2007, pp. 127-133.
- [3] Harrison, N. R., Luckey, S. G., Friedman, P. A., and Xia, Z. C., "Influence of Friction and Die Geometry on Simulation of Superplastic Forming of Al-Mg Alloys," *Advances in Superplasticity and Superplastic Forming*, E. M. Taleff, P. A. Friedman, P. E. Krajewski, R. S. Mishra, and J. G. Schroth, eds., TMS, Warrendale, PA 2004, pp. 301-309.
- [4] Verma, R., Carter, J. T., "Quick Plastic Forming of a Decklid Inner Panel with Commercial AZ31 Magnesium Sheet," *SAE Technical Paper 2006-06-0525*.
- [5] Taleff, E. M., Hector, L. G. Jr., Bradley, J. R., Verma, R., and Krajewski, P. E., "Local Thinning at a Die Entry Radius during Hot Gas-Pressure Forming of an AA5083 Sheet", *Journal Manuf. Sci. Eng.*, Vol. 132, No. 1, 2010, 011016 (7 pages).
- [6] Ghosh, A. K., Hamilton, C. H., "Superplastic Forming of a Long Rectangular Box Section—Analysis and Experiment", *Mater. Process. Congr. 1978–1979*, 1980, pp. 303-331.
- [7] Khaleel, M. A., Johnson, K. I., and Smith, M. T., "On the Thinning Profiles in Superplastic Forming of a Modified 5083 Aluminum Alloy", *Mater. Sci. Forum.*, Vols. 243-245, 1997, pp.739-744.
- [8] Luckey, G. Jr., Friedman, P. A., and Weinmann, K. J., "Correlation of Finite Element Analysis to Superplastic Forming Experiments", *Journal Mater. Process. Technol.*, Vol. 194, No. 1-3, 2007, pp. 30-37.
- [9] Hwang, Y. M., Yang, J. S., Chen, T. R., Huang, J. C., "Analysis of Superplastic Sheet Metal Forming in a Circular Closed-Die Considering Non-Uniform Thinning", *Journal Mater. Process. Technol.*, Vol. 65, Nos. 1-3, 1997, pp. 215-227.

- [10] Hwang, Y. M., Lay, H. S., and Huang, J. C., "Study of Superplastic Blow-Forming of 8090 Al-Li Sheets in an Ellip-Cylindrical Closed-Die", *Int. J. Mach. Tools Manuf.*, Vol. 42, No. 12, 2002, pp.1363-1372.
- [11] Garriga-Majo, D., Curtis, R., "Geometric Analysis of Thinning during Superplastic Forming," *Materials Science Forum*, Vols. 357-359, 2001, pp.213-218.
- [12] Lin, J., "Selection of material models for predicting necking in superplastic forming", *International Journal of Plasticity*, Vol. 19, No. 4, 2003, pp. 469-481.
- [13] Chen, Z. P., Thomson, P. F., "A study of post-form static and fatigue properties of superplastic 7475-SPF and 5083-SPF aluminum alloys", *Journal of Materials Processing Technology*, Vol. 148, No. 2, 2004, pp. 204-219.
- [14] Verma, R., Carter, J., "Quick Plastic Forming of a Decklid Inner Panel with Commercial AZ31 Magnesium Sheet", *SAE Technical Paper 2006-01-0525*.
- [15] Hector, Jr., Krajewski, P. E., Taleff, E. M., and Carter, J. T., "High-Temperature Forming of a Vehicle Closure Component in Fine- Grained Aluminum Alloy AA5083: Finite Element Simulations and Experiments", *Key Engineering Materials*, Vol. 433, 2010, pp. 197-209.
- [16] Albakri, M. I., Jarrar, F. S., and Khraisheh, M. K., "Effects of Interfacial Friction Distribution on the Superplastic Forming of AA5083," *Eng. Mater. Technol.*, Vol. 133, No. 3, 2011, 031008 (6 pages).
- [17] Balasubramanian, M., Ramanathan, K., and Sentil Kumar, V. S., "Mathematical Modeling and Finite Element Analysis of Superplastic Forming of Ti-6Al-4 V Alloy in a Stepped Rectangular Die", *International Conference on Design and Manufacturing (IConDM2013)*, Vol. 64, 2013, pp. 1209-1218.
- [18] Li, Q., "Thickness distribution of superplastic formed titanium-based domes," *JOM*, Vol. 62, No. 5, 2010, pp. 25-27.
- [19] Carrino, L., Giuliano, G., Palmieri, C., "On the Optimization of Superplastic Forming Processes by the Finite-element Method", *J. Mater. Process. Technol.*, Vols. 143-144, 2003, pp. 373-377.
- [20] Nazzal, M. A., Khraisheh, M. K., and Darras, B. M., "Finite Element Modeling and Optimization of Superplastic Forming Using Variable Strain Rate Approach," *J. Mater. Eng. Perform.*, Vol. 13, No. 6, 2004, pp. 691-699.
- [21] Khraisheh, M. K., Zbib, H. M., "Optimum Forming Loading Paths for Pb-Sn Superplastic Sheet Materials," *ASME J. Eng. Mater. Technol.*, Vol. 121, No. 3, 1999, pp. 341-345.
- [22] Albakri, M. I., Khraisheh, M. K., "Optimization of Superplastic Forming; Effects of Interfacial Friction on Variable Strain Rate Forming Paths", *Advances in Sustainable Manufacturing*, 2011, pp. 121-126.
- [23] Jarrar, F. S., Hector, L. G. Jr., Khraisheh, M. K., and Bower, A. F., "New approach to gas pressure profile prediction for high temperature AA5083 sheet forming", *Journal of materials processing technology*, Vol. 210, Nos. 6-7, 2010, pp. 825-834.
- [24] Verma, R., Hector, L. G., Krajewski, P. E., and Taleff, E. M., "The Finite Element Simulation of High-temperature Magnesium AZ31 Sheet Forming", *JOM Journal of the Minerals, Metals and Materials Society*, Vol. 61, No. 8, 2009, pp. 29-37.
- [25] Zareh, B., Gorji, A. H., Bakhshi, M. and Nourouzi, S., "Study on the effect of forming parameters in sheet hydrodynamic deep drawing using FEM based Taguchi method", *Int. Journal of Advanced Design and Manufacturing Technology*, Vol. 6, No. 1, 2013, pp. 87-99.
- [26] Luckey, S. G., Friedman, P. A., and Xia, Z. C., "Aspects of element formulation and strain rate control in the numerical modeling of superplastic forming", In: Taleff, E. M., Friedman, P. A., Krajewski, P. E., Mishra, R. S., Schroth, J.G. (Eds.), *Proceedings of Advances in Superplasticity and Superplastic Forming*. TMS (The Minerals, Metals & Materials Society), 2004, pp. 371-380.
- [27] *ABAQUS Analysis User's Manual*, Version 6.12, Vol. 3, pp. 23.2.4-10-23.2.4-11.